Indigenization of Buoy Components Using Additive Manufacturing Technique

Thirumurugan KARUPPIAH [1, 2] *, Shanmuga Sundaram KARIBEERAN [1], Murugesh POTHIKASALAM [2], Tata SUDHAKAR [2]

[1] *College of Engineering Guindy, Anna University, 12 Sardar Patel Road, Guindy, Chennai,Tamilnadu - 600 025, India*
[2] *National Institute of Ocean Technology,Velachery Tambaram Main Road, Narayanapuram, Pallikaranai, Chennai, Tamilnadu - 600 100, India*

http://doi.org/10.5755/j02.ms.34062

Received 11 May 2023; accepted 30 August 2023

The Ocean Observation Systems (OOS) group of the National Institute of Ocean Technology (NIOT) is involved in the design, development and sustenance of moored data buoys in the Indian Seas. The moored buoy systems deployed in the Northern Indian Ocean provide real-time, continuous observation of surface meteorological and oceanographic parameters which help in monitoring extreme weather events and natural disasters such as cyclones and tsunamis. Buoy components are of different sizes and shapes and are made of various materials, including metals and plastics. However, due to unique and critical design requirements, the development of deep-sea components faces hurdles caused by manufacturing limitations. The advent of additive manufacturing (AM) has met the demand for quickly producing parts. Due to the high pressure and low temperature conditions, it is extremely difficult to design and develop deep sea components. Consequently, High Impact Polystyrene (HIPS) material has been selected for the subsurface floats. The float is manufactured using the Fused Deposition Modeling (FDM) additive manufacturing technique in the Fabheads 1K FDM printer with pellet based extrusion method. These subsurface floats are used at a water depth of 500 m in NIOT buoy systems, with a working pressure of approximately 50 bar. Taking a factor of safety of two into account, the part is designed to withstand 100 bar. To assess the component's performance under deep-sea hydrostatic conditions, it underwent testing in the hyperbaric chamber test facility at NIOT. During the qualification process, the component successfully withstood the design pressure of 100 bar and imploded at 102 bar. This study is part of NIOT's ongoing efforts to indigenize deep-sea components using AM and assess its future prospects.
Keywords: buoy components, deep sea, additive manufacturing, fused deposition modeling.

1. INTRODUCTION

Since its inception in 1997, the moored buoy program has successfully sustained the buoy systems in the Northern Indian seas for more than 25 years. The moored buoys provide real time meteorological and oceanographic data sets from coastal and deep-sea locations [1]. The weather forecasting and warning systems are greatly enhanced by the systematic time series measurements of moored buoy systems, especially during extreme weather phenomena like cyclones and tsunamis. The surface buoy (floating on the water surface), instrument container, mast assembly, electronic sensors, mooring components, subsurface plastic and glass floats, and sinker weight (anchored on the sea bed) are components of the moored buoy system. These components are made of various materials, including aluminum 6061 T6, stainless steel 316, medium density polyethylene (MDPE), Polystyrene, FRP, 17- 4 PH steel, and galvanized steel. The pressure enclosure and the buoyancy floatation devices are the essential parts of the moored buoy systems. Steels, titanium, and ceramics are some of the materials used to make underwater pressure vessels, and they should be lightweight but should have high strength [2]. The buoyancy floatation units that are added to the subsea system will significantly lower its weight, causing it to become neutrally buoyant [3]. The moored buoy network as shown in Fig. 1 includes 12 deep ocean OMNI buoys, 3 coastal buoys, 4 tsunami buoys and a Cal-Val buoy.

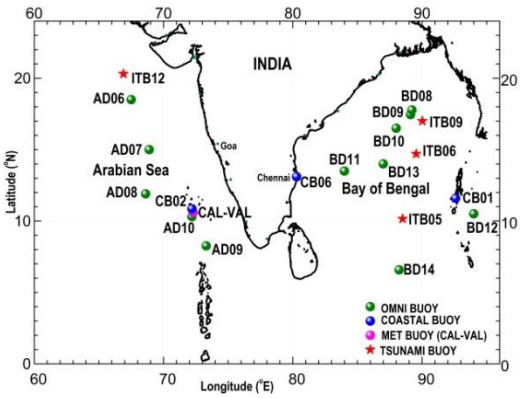

Fig. 1. Moored buoy network in the Northern Indian Ocean

Pressure enclosures can be utilized to enclose electronic instruments and power sources that are attached to the mooring line and deployed at the desired depth. Subsurface floats are employed in the mooring line to provide the necessary buoyancy for recovering the instruments from the deployed depth to the sea surface. The size of the pressure enclosure and float depends on factors such as the payload of the electronics, working depth, and buoyancy requirements.

*Corresponding author. Tel.: +91-44-66783532; fax: +91-44-66783400
E-mail: *thirumurugan@niot.res.in* (T. Karuppiah)

The conventional manufacturing process, due to high setup costs and longer lead times, is not suitable for accommodating dynamic design changes based on project requirements. However, considering the specific nature of the application and the relatively low number of components required, emerging technologies like additive manufacturing are deemed more suitable for producing underwater components. The spherical shape of the float is advantageous as it offers a streamlined body with reduced drag and the ability to withstand high hydrostatic pressures. A study has been undertaken to explore the feasibility of designing and fabricating a spherical float as an early proof of concept of being able to produce unique instrument housings using additive manufacturing. The general method of the additive manufacturing process is illustrated in Fig. 2. A 3D model is created using CAD software for slicing the designed part [4].

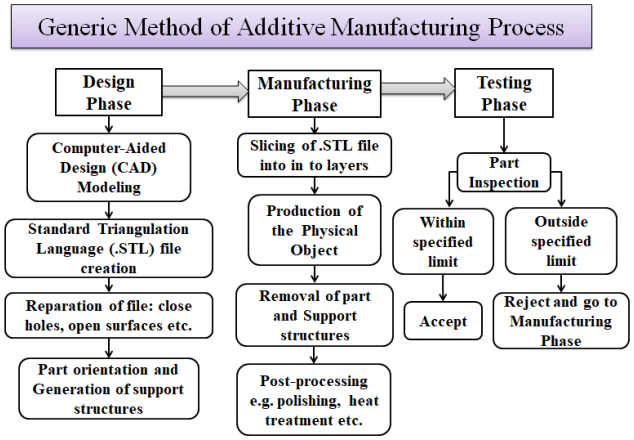

Fig. 2. Stages in additive manufacturing

The software, converted into an .STL file, and then sent to C6 components are constructed using the same additive manufacturing approach. The data preparation process involves determining the part orientation, placement of support structures, and slicing of the model. Post-processing may be conducted on the parts before testing.

Additive manufacturing involves adding individual building components one layer at a time, similar to stacking a pack of cards. The fused material is layered to form the parts, following the principles of Fused Deposition Modeling (FDM).

Deep-sea buoy components typically require high-strength materials to withstand the extreme pressure conditions in the water column. The high hydrostatic pressure experienced alters the yield criterion of the materials. Designing and operating deep-water systems pose significant challenges and necessitate thorough testing before implementation.

2. MATERIALS AND METHODS

As part of the indigenization of the moored buoy components, the subsurface float was designed with plastic material and fabricated with 3D printing technology. A polymer based High-Impact Polystyrene (HIPS) was chosen for our application and has been gaining more and more attention in additive manufacturing. HIPS is more suitable for our application compare to other materials due to good adhesion and its resistance to warping. HIPS is a thermoplastic polymer with spheroid domains embedded in an amorphous polystyrene matrix, with better opacity, elongation, plasticity, and energy absorption properties. It is usually obtained as a result of the free radical polymerization of styrene monomer in the presence of rubbers, usually polybutadiene (PB), to enhance the impact strength and toughness of polystyrene (PS) [5]. Depending on the rubber particle size and the number of occlusions, two typical morphologies are usually identified as a 'salami morphology' (large rubber particle with several occlusions) or a 'core–shell morphology' (relatively small rubber particle with only one large occlusion), which provide the material with improved mechanical properties [6, 7].

They have much higher qualities than standard thermoplastics, including flexibility, breakage resistance, and simplicity of processing. Since it has high impact strength and a low tensile strength, it is excellent for structural applications. Several studies have been done on material [8]. The static and dynamic behavior of HIPS material demonstrates its ductility [8, 9].

It was concluded that PS is brittle but the toughness is increased sufficiently when it is blended with rubbers. Rubber inclusions induce plastic deformation to the matrix which absorbs energy giving higher toughness and ductility to HIPS [9]. The stress strain curves and strain hardening rate curve of HIPS are shown in Fig. 3.

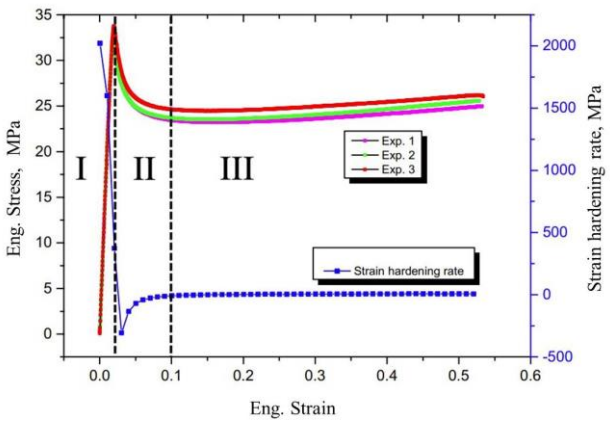

Fig. 3. Static stress-strain and strain hardening curves for HIPS

The stress-strain curves of HIPS under strain rate ranging from 0.001 to 100 s^{-1} are shown in Fig.4.

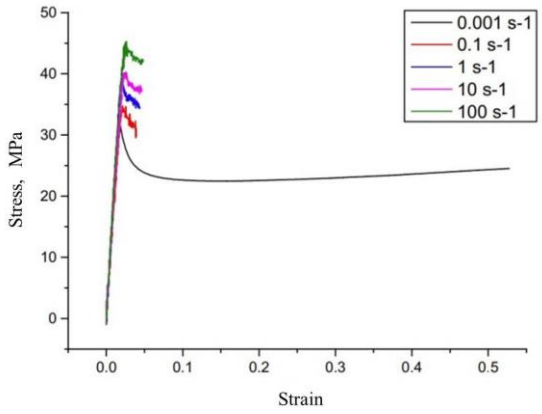

Fig. 4. Stress-strain curves for HIPS material at strain rate range of 0.001 to 100 s^{-1} [8]

Three deformation stages can be identified: stage-I as the elastic region corresponding to strain level of 0 – 0.02, stage-II as strain softening region with 30 % reduction in stress corresponding to strain level of 0.02 – 0.1 and stage-III as the strain hardening region corresponding to strain level of 0.1 up to the strain at final fracture [8].

Based on Fig. 3 and Fig. 4, it is inferred that the yield strength of the HIPS material is considered as 31 MPa. Some of the important mechanical and thermal properties of HIPS are given in Table 1.

Table 1. General mechanical and thermal properties of HIPS [8, 10]

Properties	Values
Density ρ	1040 kg/m^3
Young's modulus E	1.9 GPa
Poisson ratio ν	0.41
Yield strength σ_y	31 MPa
Thermal conductivity κ	0.3 W/m-K
Coefficient of thermal expansion α	80 µm/m-K
Specific heat C_p	1400 J/kg-K

Spherical floats made of HIPS material were created using the Fused Deposition Modeling (FDM) additive manufacturing technique. This was accomplished by using an open-build Fabheads 1K FDM printer, as shown in Fig. 5. Among the various 3D printing processes, one of the most commonly used technologies is FDM. FDM extrudes a thin bead of plastic layer one at a time to make a part. A thread of plastic is fed into an extrusion head where it is heated into a semi-liquid state and extruded through a very small hole onto the support material or the previous layer of the plastic. The spherical float as a single piece can only be produced using FDM because using this method we can make a single spherical float without internal support material whereas in other additive manufacturing technologies we need to split up the components because of the internal support creation. The main advantages of this technology include a good variety of available materials, easy material change, low maintenance costs, quick production of thin parts, overall tolerance up to 0.1 mm, no need for supervision, very compact size and low temperature operation.

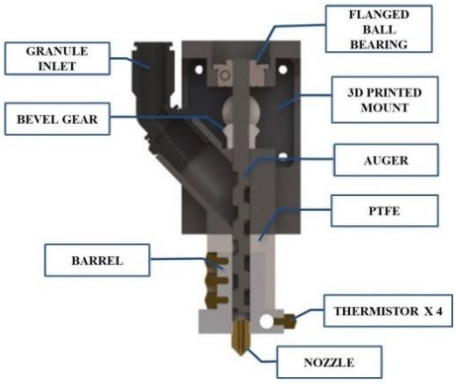

Fig. 5. Schematic of open-build Fabheads 1K FDM printer [11]

The disadvantages of using FDM include rough surface finish, slow processing speed and limitations on achievable dimensions, leading to quality issues and poor aesthetics. Additionally, when removing the supports from the components, blemishes may be formed.

3. MATHEMATICAL MODEL

Spherical pressure vessels can withstand very high-pressure fluids. It has approximately twice the strength of a cylindrical pressure vessel with the same wall thickness [12]. The spherical pressure vessels however, are costlier to manufacture than cylindrical vessels.

The yield pressure (P_{yield}) of a thick spherical pressure float is given by Zhang et. al, Eq. 1.

$$P_{yield} = \frac{4t\sigma_y}{D_m}, \tag{1}$$

where σ_y is the yield strength of a material; D_m is the mean diameter of the sphere, and t is the spherical shell thickness [13, 14]. As per the requirements, the float is designed to the specifications at a working depth of 500 m (~ 50 bar), with a safety factor of two.

This results in a net external pressure on the float of 10.06 MPa, with a seawater density of 1025 kg/m^3. It is calculated that the minimum required thickness is ~ 19 mm. As a general rule, pressure vessels are considered to be thick-walled when the ratio of diameter (d) to wall thickness (t) is less than 20. The float was designed and shell thickness was calculated based on mathematical relations and fabricated using 3D printing FDM technology. The spherical float made by 3D printing was meant to have an inner diameter of 216 mm and a thickness of 19 mm. However, due to the manufacturing limitation of the process, the part also underwent a post-processing step to reach the desired final dimension.

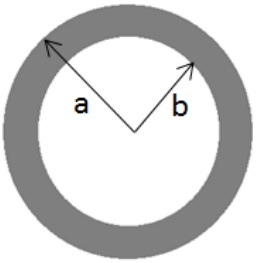

Fig. 6. Schematic representation of the spherical float with inner and outer radii manufactured by FDM process

The stress field in the thick spherical shells is given by Eq. 2 and Eq. 3, where σ_r and σ_θ are radial and tangential stresses respectively [13]:

$$\sigma_r = \frac{E}{(1+\nu)(1-2\nu)}\left[(1+\nu)C_1 - 2(1-2\nu)\frac{C_2}{r^3}\right]; \tag{2}$$

$$\sigma_\theta = \frac{E}{(1+\nu)(1-2\nu)}\left[(1+\nu)C_1 + (1-2\nu)\frac{C_2}{r^3}\right]. \tag{3}$$

The boundary conditions for the outer pressure loading are as follows:

$$\text{At } r = a, \sigma_r = -P; \tag{4}$$

$$\text{At } r = b, \sigma_r = 0, \tag{5}$$

where a and b are the outer and inner radii of the sphere respectively as shown in Fig. 6. Also, P is the applied external pressure and on substitution of the prescribed

boundary condition Eq. 4 and Eq. 5 in Eq. 2 and Eq. 3, the constants C_1 and C_2 are obtained as follows:

$$C_1 = \frac{-Pa^3}{E(a^3-b^3)}(1-2\nu); \quad (6)$$

$$C_2 = \frac{-Pa^3b^3}{2E(a^3-b^3)}(1+\nu). \quad (7)$$

After substituting the values of C_1 and C_2 in Eq. 2 and Eq. 3, obtained the final radial and tangential stresses at the outer and inner surface as:

At $r = a$

$$\sigma_r = -P$$
$$\sigma_\theta = -\frac{1}{2}\frac{P(2a^3+b^3)}{(a^3-b^3)} \quad (8)$$

At $r = b$

$$\sigma_r = 0$$
$$\sigma_\theta = -\frac{3}{2}\frac{Pa^3}{(a^3-b^3)} \quad (9)$$

As a result, the spherical floats will experience the following radial and tangential stresses Table 2.

Von Mises yield criterion at the onset of yield is given as Eq. 10 [13] where, $\sigma_{v,m}$ is the von Mises equivalent stress and σ_y is the yield stress.

$$\sigma_{v,m} = \sigma_y = |\sigma_r - \sigma_\theta|. \quad (10)$$

Table 2. Radial and tangential stresses on the spherical float for the given external pressure of 10.06 MPa

Radial stress $\boldsymbol{\sigma_r}$, MPa		Tangential stress $\boldsymbol{\sigma_\theta}$, MPa	
Inner surface	Outer Surface	Inner surface	Outer surface
0	-10.06	-39.17	-34.14

4. NUMERICAL MODEL

The finite element method is a highly effective tool for conducting stress analysis on engineering structures. It enables us to closely approach the actual solution by incorporating real engineering problems into the analysis. Analytical models, which involve equations or formulas, are commonly employed to estimate the stress state in a structure. These models are derived from fundamental principles and assumptions. By comparing the analytical predictions with numerical simulation results, the accuracy and reliability of the analytical models can be verified. Discrepancies or deviations between the two sets of data can indicate the necessity for adjustments or enhancements to the analytical approach.

To validate the proposed analytical solution, an axisymmetric finite element model of the spherical vessel is shown in Fig. 7 a was constructed in FEA software, ANSYS. Converged meshes of a total of 10560 elements were generated. The material properties and boundary conditions were implemented the same as the analytical model. Due to mechanical loading, the buoy components are experiencing a compressive stress state in the vessel wall and the minimum and maximum stress values of half model of the 2D axisymmetric sphere are shown in Fig. 7 b. This is the material response as the result of the inner wall of the vessel being subjected to higher pressure compared to the outer wall of the vessel. The Von Mises stresses are calculated and compared with the analytical solution as shown in Table 3.

Substituting the values of radial and tangential stress from Table 2 in Eq. 10, the Von Mises stresses are calculated and the numerical results from ANSYS are shown in Table 3.

Table 3. Comparison of analytical and numerical results

Von Mises stress $\sigma_{v,m}$, MPa	Analytical results	Numerical results
Inner surface	39.174	39.176
Outer surface	24.091	24.089

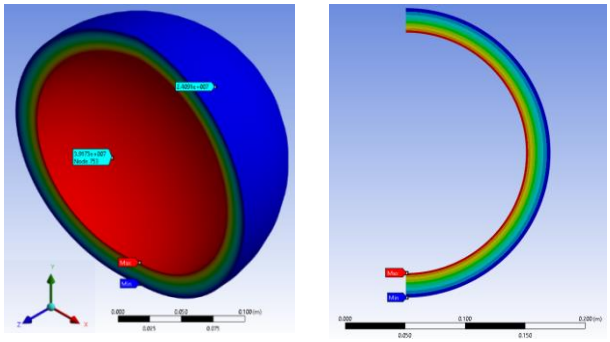

a b

Fig. 7. a – 2D section of axisymmetric spheres; b – half model of the sphere showing minimum and maximum stress

It is observed from the table, that the results obtained from both techniques are in accordance with each other, instilling confidence in progressing towards production.

5. MANUFACTURING METHOD

There are two types of FDM processes: filament-based and pellet-based. The float was printed using pellet technology with the Fabheads 1K machine Fig. 8. This technology allows for the rapid deposition of a large amount of material, making it suitable for large-scale 3D printing. Both the part and support material were built using the same material, utilizing a single extruder nozzle. The printer specifications and print settings can be found in Table 4 and Table 5 respectively.

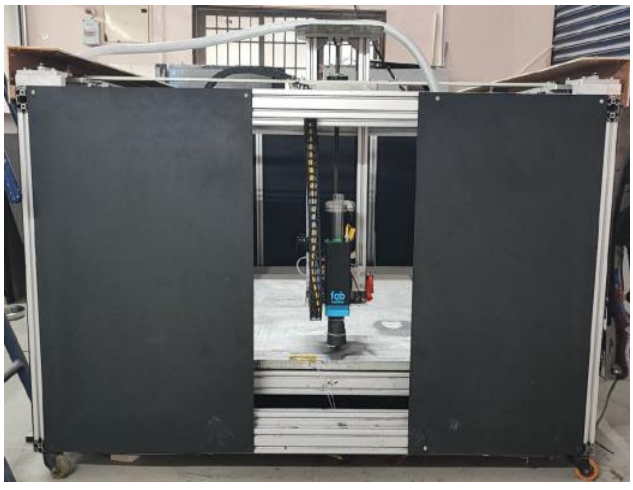

Fig. 8. FDM Printer FABHEAD-1K

Table 4. FDM Print specifications

Specifications	Details
Build volume	1000 × 1000 × 1000 mm
Nozzle diameter	4 mm
Pellet diameter	2 – 3 mm granules
Enclosure	Top Open Enclosure
Extruders	1 air cooled
Max extruder temperature	500 °C
Heated bed/max bed temperature	120 °C
Bed material	Tool aluminum
Material format	Pellets size < 4 mm

Regarding post-processing, the following steps were undertaken: Firstly, supports were manually removed using tools such as a spatula, chisel, and cutter. Next, over-projected and uneven surfaces, such as burrs and blobs, were smoothed out using sanding paper to achieve a polished finish.

Table 5. FDM Print settings

Settings	Details
Printing speed	70 mm/s
Height of layer	2 mm
Fill pattern	Concentric
Extrusion temperature	230 °C
Print bed temperature	80 °C
Infill percentage	100 %
Support structure details	Zig zag pattern (20% of density)
Support material	HIPS
Build time	6 hours 36 minutes

Coatings like gel coat, resin coat, and powders were then applied to enhance the aesthetics of the float. Finally, the float was painted with two coats of epoxy anti-corrosive primer pigmented with zinc phosphate, along with one top coat of acrylic polyurethane paint was applied to the external surface of the float.

6. EXPERIMENTAL RESULTS

The 3D printed float is shown in Fig. 9. Dimensional accuracy of the 3D printed spherical float is inspected by measuring the thickness [16] using TT100 Ultrasonic Thickness Gauge Fig. 10 a. The thickness of the spherical shell was found to be $19^{+0.4}_{-0.2}$mm. The theoretical mass of the float was calculated as 3.43 kg whereas the actual mass was measured as 3.6 kg. The difference in the mass value is due to the actual thickness of the float, which was not constant throughout the entire diameter. The buoyancy of the float was 5.15 kg.

Roundness of the 3D printed spherical float was measured using an vernier height gauge with a dial indicator Fig. 10 b and it was found to vary within a range of +0.8 mm and -0.4 mm of diameter, due to post processing and painting.

A hyperbaric chamber is a device that simulates the underwater pressure environment with its pressure-resistant structure. NIOT has a hyperbaric test facility for testing underwater systems with external pressure up to 900 bar (~9000 m water depth). This facility is the first of its kind in India. A hyperbaric chamber is essential for the development of underwater equipment, as it enables the validation of deep-sea components in a more efficient and cost-effective manner than conducting actual tests in the deep sea.

Fig. 9. 3D printed spherical float manufactured by FDM process

a b

Fig. 10. a – thickness measurement using TT100 Ultrasonic Thickness Gauge; b – roundness measurement of the float using Vernier Height Gauge with a dial indicator

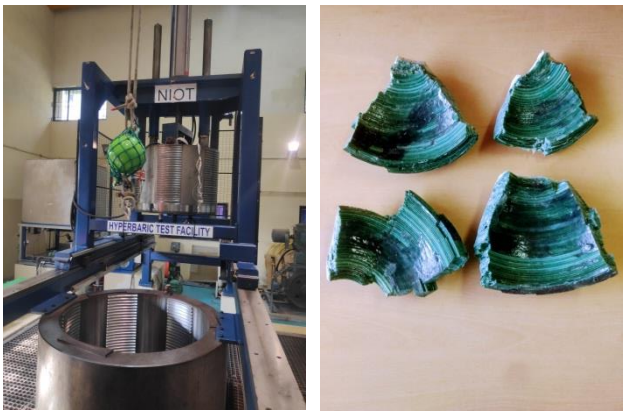

a b

Fig. 11. a – hyperbaric test of the float; b – imploded 3D printed float after hyperbaric test

The hyperbaric test for the 3D-printed float was conducted at NIOT, as depicted in Fig. 11 a. The pressure was gradually raised in 10-bar increments, starting from 1 bar and reaching the design pressure of 100 bar. At each increment, the pressure was kept constant for two minutes, up to 40 bars. To verify that the required working pressure was achieved, the pressure was continuously maintained at 50 bar for 15 minutes. Subsequently, the pressure was held constant for two minutes at each increment from 60 bar to 90 bar. To ensure compliance with the design pressure requirement, the pressure was maintained at 100 bar for 15 minutes. The pressure was then further increased to assess the float's maximum pressure resistance capacity. However, the float eventually imploded at a pressure of

102 bar (~1040 m water depth), as shown in Fig. 11 b.

7. CONCLUSIONS

The yielding of spherical floats under external pressure is discussed through analytical and numerical studies using ANSYS software. By applying external hydrostatic pressure to a spherical float, it was found that the yielding process begins at the inner surface of the sphere. Von-Mises stresses were calculated both analytically and numerically, and the results obtained from both methods were in good agreement. The float, made of HIPS material and manufactured using newer emerging technology like 3D printing with the FDM method, has a larger scope for improvement in underwater applications. It can be indigenized for further buoy components required to withstand high pressure ratings. This innovative concept will be expanded to include spherical shells of varying thicknesses under higher external pressures (corresponding to higher water column depths) for a variety of underwater applications such as buoyancy floats and instrument housings.

Acknowledgments

The authors would like to express their gratitude to the Ministry of Earth Sciences, Government of India, for funding the Ocean Observation Network program, and to the members of the National Expert Committee for their contributions to this program. We would also like to thank the Director of NIOT for providing us with all the necessary facilities and encouragement. Additionally, we extend our thanks to the staff of the Ocean Observation Systems group for their invaluable assistance and support.

REFERENCES

1. **Venkatesan, R., Lix, J.K., Phanindra Reddy, A., Arul Muthiah, M., Atmanand, M.A**. Two Decades of Operating the Indian Moored Buoy Network: Significance and Impact *Journal of Operational Oceanography* 9 (1) 2016: pp. 45 – 54. https://doi.org/10.1080/1755876X.2016.1182792
2. **Takagawa, S.** New Ceramic Pressure Hull Design for Deep Water Applications *In OCEANS'10 IEEE SYDNEY, IEEE* 2010: pp. 1 – 6. https://doi.org/10.1109/OCEANSSYD.2010.5603796
3. **Breddermann, K., Drescher, P., Polzin, C., Seitz, H., Paschen, M.** Printed Pressure Housings for Underwater Applications *Ocean Engineering* 113 2016: pp. 57 – 63. https://doi.org/10.1016/j.oceaneng.2015.12.033
4. **Jiménez, M., Romero, L., Domínguez, I.A., Espinosa, M.D.M., Domínguez, M.** Additive Manufacturing Technologies: an Overview About 3D Printing Methods and Future Prospects *Complexity* 2019: p. 30. https://doi.org/10.1155/2019/9656938
5. **Sieradzka, M., Fabia, J., Biniaś, D., Graczyk, T., Fryczkowski, R.** High-Impact Polystyrene Reinforced with Reduced Graphene Oxide as a Filament for Fused Filament Fabrication 3D Printing *Materials* 14 2021: pp. 7008. https://doi.org/10.3390/ma14227008
6. **Maffi, J.M., Estenoz, D.A.** On the Evolution of Particle Size Distributions During the Bulk Synthesis of High-Impact Polystyrene Using PBM: Towards Morphology and Phase Inversion Prediction *Chemical Engineering Science* 247 2022: pp. 117027. https://doi.org/10.1016/j.ces.2021.117027
7. **Wang, F., Chang, L., Hu, Y., Wu, G., Liu, H.** Synthesis and Properties of In-Situ Bulk High Impact Polystyrene Toughened by High Cis-1, 4 Polybutadiene *Polymers* 11 (5) 2019: pp. 791. https://doi.org/10.3390/polym11050791
8. **Fu, S., Wan, Z., Lu, W., Liu, H., Zhang, P.E., Yu, B., Liu, Z.** High-Accuracy Virtual Testing of Air Conditioners Digital Twin Focusing on Key Material's Deformation and Fracture Behaviour Prediction *Scientific Reports* 12 2022: pp. 12432 https://doi.org/10.1038/s41598-022-16511-w
9. **GENÇER, A.** Design of Rigid Wheat Gluten Materials Improved Mechanical Properties by Blending with Polyamides, *Master of Science thesis, KU Leuven* 2014.
10. **KHLIFA, S.B., Lammari, L., Kharroubi, H.** Experimental and Numerical Modelling the Effect of the Residual Stress in the Case of the Molding of a Plastic Part *Materiale Plastice* 58 (2) 2021: pp. 60 – 70. https://doi.org/10.37358/MP.21.2.5478
11. **Drotman, D., Diagne, M., Bitmead, R., & Krstic, M.** Control Oriented Energy Based Modelling of a Screw Extruder Used for 3D Printing *Proceedings of the ASME2016 Dynamic Systems and Control Conference* V002T21A002, 2016. https://doi.org/10.1115/DSCC2016-9651
12. **Fryer, D.M., Harvey, J.F.** High Pressure Vessels. *Springer Science + Business Media Dordrecht*, 1998.
13. **Kholdi, M., Loghman, A., Ashrafi, H., Arefi, M.** Analysis of Thick-Walled Spherical Shells Subjected to External Pressure: Elastoplastic and Residual Stress Analysis. Proceedings of the Institution of Mechanical Engineers, Part L: *Journal of Materials: Design and Applications* 234 (1) 2020: pp. 186 – 197. https://doi.org/10.1177/1464420719882958
14. **Pranesh, S.B., Sathianarayanan, D., Ramadass, G.A.** Design Standards for Steel Spherical Pressure Hull for a Manned Submersible *Journal of Ocean Engineering and Marine Energy* 8 (2) 2022: pp. 137 – 151. https://doi.org/10.1007/s40722-021-00221-y
15. **Wang, C.M., Wang, C.Y.** Exact Solutions for Buckling of Structural Members. *CRC Press*. 2004.
16. **Zhu, Y., Guan, W., Wang, H., Zhao, M., Zhang, J.** Buckling of Spherical Shells with Pitting Corrosion under External Pressure *Ships and Offshore Structures* 17 (11) 2021: pp. 2470 – 2479. https://doi.org/10.1080/17445302.2021.2000266
17. **Muthuvel, P., Maurya, S., Sudhakar, T.** Development of Autonomous Underwater Profiling Drifter (AUPD) and field results *Journal of Earth System Science* 132 (11) 2023: pp. 1 – 13. https://doi.org/10.1007/s12040-022-02029-2